SIMULATED PLASMA AT X AND K BANDS

By S. K. CHATTERJEE, (Mrs.) R. CHATTERJEE AND D. V. GIRI

(Department of Electrical Communication Engineering, Indian Institute of Science, Bangalore-12 India)

[Received : May 2, 1970]

ABSTRACT

Wire-grid structures made of copper and resistance wires have been used to simulate the behaviour of lossless and lossy plasma respectively under the influence of microwave radiation at X and K bands. Expressions for equivalent electron density (N), transmission (t_w) *aud reflection* (ρ_w) *coefficients have been derived in terms of spacing* (a) *between wires and spacing* (b) *between structures placed in the direction of propagation. The coefficients* t_w *aud* ρ_w *and impedance characteristics, and equivalent inductive component have been calculated as functions of* b *and* a *by utilising the concept of transmission line analogue of an actual plasma. Experimental results on the shift of the angular position of major lobe due to interaction between microwave radiation and the simulated plasma have been utilised to calculate N and effective dielectric constant as functions of* b *and* a.

1. INTRODUCTION

Microwave electronic devices such as beam-plasma amplifier, phase shifter, etc. have been developed as a result of the study of inter-action phenomena between plasma and microwaves. A proper understanding of the propagation characteristics of microwave through plasma is essential for the success of space communication. The frequent failure of signal transmission during launching or re-entry of space vehicles has stimulated microwave investigations on the transmission ability of the plasma medium created on a laboratory scale as a function of electron density, frequency and angle of incidence of the incident wave. However, a laboratory study of the phenomena of interaction of actual plasma with electromagnetic wave is associated with difficulties and uncertainties of the creation of a homogeneous, stable plasma and also a plasma medium large enough to avoid diffraction effects. Moreover, in the case of a laboratory plasma, the plasma sheath is nonuniform and bounded and hence the solution of Maxwell's equation for the actual geometry of the plasma sheath usually leads to intractable mathematics which do not lead to simple physical interpretation. It is rather convenient to consider the plasma as a dielectric medium whose behaviour may be described by the following permittivity tensor ϵ_{ik}

$$\epsilon_{ik} = \epsilon_0 \begin{Bmatrix} \epsilon_1 & -i\epsilon_2 & 0 \\ i\epsilon_2 & \epsilon_1 & 0 \\ 0 & 0 & \epsilon_3 \end{Bmatrix} \qquad [1]$$

where, the ionic motion in the X and K bands is disregarded in a constant magnetic field directed along the z-axis, and the different components depend appropriately on signal angular frequency ω, electron plasma angular frequency ω_p, electron angular gyrofrequency ω_H and effective frequency ν_{eff} of electron collision.

The actual plasma can be simulated by electromagnetic structures such as parallel plate media and wire-grid whose effective dielectric constant is less than unity. The properties of reflection and transmission of such structures have been studied by Carlson and Heins[1], Chatterjee, *et al*[2,3], Wait[4], Brown[5], Macfarlane[6], Ignatowsky[7,8], and Skwirzyris[9]. It is known that the radiation pattern of an antenna undergoes modifications in structure as well as in angular position of lobes when it passes through a plasma medium. The present investigation is concerned with the artificial simulation of plasma at X and K bands by wire-grid with the object of determining the electron density of a corresponding actual plasma so that the radiation pattern of a microwave horn in the presence of plasma can be predicted. Two types of structures *viz*, single wire-grid which may be called Y plasma and crossed wire-grid which may be called X Y plasma have been used to simulate plasma. Loseless and lossy plasma have been simulated by using copper and resistance wires respectively for the construction of grid structures. The paper forms a part of the work on artificial dielectrics[2,3,10,11,12] at microwave frequencies.

2. Equivalent Circuit of a Plasma

In a homogeneous, isotropic, loss-free, source-free and simple medium, the electric $\vec{E}$ and the magnetic $\vec{H}$ field vectors having harmonic time dependence $\exp(j\omega t)$ for plane waves $[(\partial/\partial x)=0,\ (\partial/\partial y)=0]$ propagated along z-direction in free space are related by the following differential equations

$$(dE/dx) = -j\omega\mu_0 H, \qquad (dH/dx) = j\omega\epsilon_0 E \qquad [2]$$

where, μ_0 and ϵ_0 represent the permeability and permittivity respectively of free space medium.

When an electromagnetic wave is propagated through a plasma medium having electron density N, the motion of electrons of charge e and mass m

under the influence of the incident electric field E gives rise to convection current density $-jNe^2E/\omega m$. The contribution to current due to ionic motion is negligibly small due to the ions having mass much greater than that of electrons. Hence disregarding the ionic component of the current, the differential equations governing E and H fields, when the wave is propagated through a plasma medium are

$$\left.\begin{aligned}(dE/dx) &= -j\omega\mu_0 H\\ (dH/dx) &= [j\omega\epsilon_0 + (Ne^2/j\omega m)]\,E\end{aligned}\right\} \quad [3]$$

The differential equations governing the voltage V and current I in a lossless transmission line having inductance L per unit length and capacitance C per unit length are given in the absence and presence of conduction current respectively as follows :

$$(dV/dx) = -j\omega LI, \quad (dI/dx) = j\omega CV \qquad [4]$$

and $$(dV/dx) = -j\omega LI, \quad (dI/dx) = [j\omega C + (1/j\omega L)]\,V \qquad [5]$$

The identical nature of the above four sets of differential equations [3,4,5] establishes the equivalence between the field and circuit theories. The equivalence is also justified from the basic definitions of voltage V and current I in terms of the line integrals of E and H respectively as

$$V = \int \vec{E}\cdot d\vec{l} \quad \text{and} \quad I = \oint \vec{H}\cdot d\vec{l} \qquad [6]$$

The analogy between the differential equations [3–6] lead to the following conclusions :

(i) The displacement current density $j\omega\epsilon_0 E$ in free space is equivalent to the current $j\omega CV$ in the capacitor C.

(ii) The energy density $\frac{1}{2}\mu_0 H^2$ stored in the magnetic field is equivalent to the energy density $\frac{1}{2}LI^2$ stored in an inductance L.

(iii) The electromagnetic wave propagation through a plasma can be treated as a network problem, where, the equivalent network consists of a series inductance $L_s = \mu_0$ with a shunt network consisting of a capacitance $C_p = \epsilon_0$ and inductance $L_p = m/Ne^2$ in parallel.

(iv) If the plasma is considered to be lossy i.e. when the collision between particles is taken into account, the term $Ne^2/j\omega m$ is modified ard an additional term $m\nu/Ne^2$ representing an equivalent resistance R is to be added in series with L_p. The equivalent network for a lossy plasma is represented in Fig. 1.

(v) The displacement current $j\omega\epsilon_0 E$ and the convection current $-jNe^2 E/m\omega$ being in antiphase, the plasma behaves as a dielectric medium

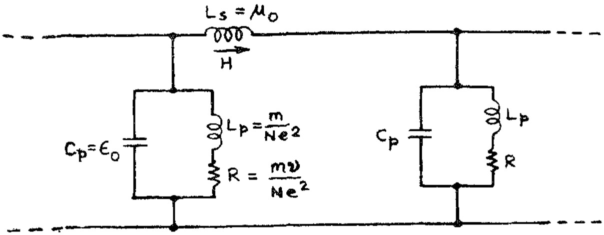

FIGt 1

Equivalent trassmission line network for a Lossy plasma.

having a permittivity $\epsilon_0 (1 - Ne^2/m\omega^2)$, when the collision is disregarded. This shows that the plasma medium can be regarded as a dielectric having dielectric constant less than unity. If the collision frequency ν is taken into account, the permittivity ϵ of the lossy plasma is given by the relation

$$\epsilon = \epsilon_0 \left(1 - \frac{Ne^2}{m(\omega^2 + \nu^2)} \right) = \epsilon_0 \left(1 - \frac{\omega_p^2}{\omega^2 + \nu^2} \right) \qquad [7]$$

which also leads to the dielectric constant of plasma to be less than unity. The plasma angular frequency ω_p is given by the relation $\omega_p^2 = (Ne^2/m)$.

The concept of the plasma as a network leads to the impedance η [13,14] of a lossless and lossy plasma respectively as

$$\eta_1 = \left[\frac{\mu_0}{\epsilon_0 (1 - \omega_p^2/\omega^2)} \right]^{1/2} = \frac{376.7}{[1 - (\omega_p^2/\omega^2)]^{1/2}} \text{ ohms} \qquad [8]$$

and

$$\eta_2 = \left[\frac{\mu_0}{\epsilon_0 [1 - \omega_p^2/\omega^2 + \nu^2)]} \right]^{1/2} = \frac{376.7}{[1 - \omega_p^2/(\omega^2 + \nu^2)]^{1/2}} \text{ ohms} \qquad [9]$$

It is evident that the convection current $-jN\epsilon^2 E/m\omega$ increases with increase of the plasma density N. If the density N increases such that it approaches the value $m\omega^2/e^2$, then $\omega_p \rightarrow \omega$. In this case, for a collision free plasma ($\nu = 0$), the intrinsic impedance $\eta_1 \rightarrow \infty$. This means that for a overdense plasma, the impedance η_1 is very high. If $\eta_1 > > \eta_0 [= \sqrt{(\mu_0/\epsilon_0)}]$ the free space impedence, the reflection coefficient will be approaching unity. Consequently, under overdense condition a plasma medium may become opaque to microwaves. This may possibly be one of the reasons for the signal blackout during the launching or re-entry of space vehicles.

3. Impedance of Simulated Plasma

The simulated plasma should not only have its relative permittivity less than unity but also should satisfy the relation

$$\eta_w/\eta_0=\gamma_0/\gamma_w \qquad [10]$$

where, $\eta_0=376.7$ ohms, $\gamma_0=\sqrt{(\mu_0\epsilon_0)}$, and η_w and γ_w represent respectively the impedance and propagation constant of the simulated plasma. The impedance η_w of the grid structure (Fig. 2) immersed in free space is given by the relation[15]

$$\eta_w=\eta_0\frac{\tan(\pi b/\lambda_0}{\tan(\pi nb/\lambda_0} \qquad [11]$$

where, b represents the spacing between grids in the direction z of propagation and a represents the spacing between wires in a grid. The refractive index n of the simulated plasma calculated in terms of the structure dimensions is given by the following relation[15]

$$n=\frac{\lambda_0}{2\pi b}\arccos\left[\cos\frac{2\pi b}{\lambda_0}+\frac{\lambda_0\sin(2\pi b/\lambda_0)}{2a\left\{ln(a/2\pi d)\cos\theta+F(a/\lambda_0,\theta)\right\}}\right] \qquad [12]$$

The correction factor $F(a/\lambda_0,\theta)$ has been evaluated by Macfarlane[6] for angles of incidence $\theta=0°$ to $\theta=90°$ and normalised spacing $(a/\lambda_0)=0.1$ to $(a/\lambda_0)=0.8$.

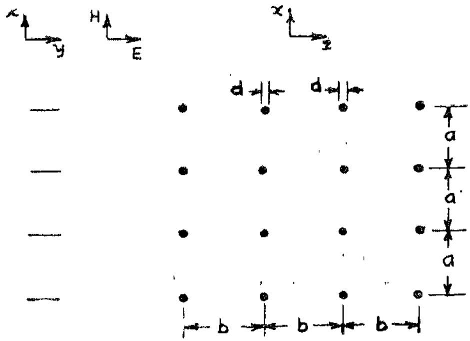

FIG. 2

Wire grid structure: **a=spacing between wires**
b=spacing between grids.

Wait[4] has derived a general expression for the function $F(a/\lambda_0, \theta)$ as follows :

$$F(a/\lambda_0, \theta) = \tfrac{1}{2}[f(\theta) + f(-\theta)] \tag{13}$$

where,

$$f(\theta) = \sum_{n=1}^{\infty} \frac{1}{n}\left[\left(\frac{n\lambda_0}{a}\right)(\sin^2\psi_n^+ - 1)^{-1/2} - 1\right] \tag{14}$$

$$\sin\psi_n^+ = \sin\theta + (n\lambda_0/a) \tag{15}$$

The reactance X_g of the structure made of wire having diameter d can be evaluated from the following expression

$$X_g = \frac{\eta_0 a}{\lambda_0}\left[ln\left(\frac{a}{2\pi d}\right)\cos\theta + F\left(\frac{a}{\lambda_0}, \quad \theta\right)\right] \tag{16}$$

which reduces to

$$X_g \cong \frac{\eta_0 a}{\lambda_0}\left[ln\left(\frac{a}{2\pi d}\right)\cos\theta\right] \tag{17}$$

when $\qquad a \leqslant 0.20\,\lambda_0$

in which case $F[a/\lambda_0, \theta] < 0.1$ for all values of the angles of incidence θ. The free space vavelength is λ_0.

4. Reflection and Transmission Coefficients of Simulated Plasma

The reflection coefficient ρ_w of the simulated plasma is obtained from equation [11] by using transmission line analogy as follows

$$\rho_w = \frac{\eta_w - \eta_0}{\eta_w + \eta_0} = \frac{\tan(\pi b/\lambda_0) - \tan(\pi nb/\lambda_0)}{\tan(\pi b/\lambda_0) + \tan(\pi nb/\lambda_0)} \tag{18}$$

The transmission coefficient t_w of the simulated plasma is obtained from equation [18] as follows

$$t_w = 1 - |\rho_w| = \frac{2\tan(\pi nb/\lambda_0}{\tan(\pi b/\lambda_0) + \tan(\pi nb/\lambda_0)} \tag{19}$$

where, the refractive index n is obtained from the relation [12]

5. Reflection and Transmission Coefficients of an Actual Plasma

The reflection ρ_p and transmission t_p coefficients of an actual lossless plasma medium are obtained from equation [8].

$$\rho_p = \frac{1-(1-\omega_1^2)^{1/2}}{1+(1-\omega_1^2)^{1/2}} \quad [20]$$

and

$$t_p = \frac{2\,(1-\omega_1^2)^{1/2}}{1+(1-\omega_1^2)^{1/2}} \quad [21]$$

where,

$$\omega_1^2 = \omega_p^2 \mid \omega^2$$

Similarly, for a lossy plasma, the refleetion ρ_{pl} and trnsmission t_{pl} coefficients are obtained from equation [9]

$$\rho_{pl} = \frac{1-(1-\omega_2^2)^{1/2}}{1+(1-\omega_2^2)^{1/2}} \quad [22]$$

$$t_{pl} = \frac{2\,(1-\omega_2^2)^{1/2}}{1+(1-\omega_2^2)^{1/2}} \quad [23]$$

where,

$$\omega_2^2 = \omega_p^2/(\omega^2+\nu^2)$$

6. Equivalent Electron Density

In order that the wire grid structure may simulate an actual plasma, the dimensional parameters of the structure should be so adjusted that its reflection and transmission properties should be the same as that of an actual plasma. Or in other words, ρ_w and t_w should be equal to ρ_p and t_p respectively in the case of a lossless plasma and equal to ρ_{pl} and t_{pl} in the case of a lossy plasma. This requires that the following relations should be satisfied

$$\frac{1-x^{1/2}}{1+x^{1/2}} = \frac{\tan(\pi b/\lambda_0)-\tan(\pi nb/\lambda_0)}{\tan(\pi b/\lambda_0)+\tan(\pi nb/\lambda_0)} \quad [24]$$

$$\frac{x^{1/2}}{1+x^{1/2}} = \frac{\tan(\pi nb/\lambda_0)}{\tan(\pi b/\lambda_0)+\tan(\pi nb/\lambda_0} \quad [25]$$

in the case of lossless plasma and

$$\frac{1-y^{1/2}}{1+y^{1/2}} = \frac{\tan(\pi b/\lambda_0)-\tan(\pi nb/\lambda_0)}{\tan(\pi b/\lambda_0)-\tan(\pi nb/\lambda_0)} \quad [26]$$

$$\frac{y^{1/2}}{1+y^{1/2}} = \frac{\tan(\pi nb/\lambda_0)}{\tan(\pi b/\lambda_0)+\tan(\pi nb/\lambda_0)} \quad [27]$$

in the case of lossy plasma, where,

$$x=(1-\omega_1^2) \text{ and } y=(1-\omega_2^2)$$

The refractive index n is obtained in terms of structure dimensions, a, b and d from the relation [12]. An expression for the equivalent plasma density N can be derived by using the equations [24] and [25] and the relation $\omega_p^2=Ne^2/m$ in the case of a lossless plasma and is given by

$$N=\frac{m\omega^2}{e^2}\left[1-\frac{\tan^2(\pi nb/\lambda_0)}{\tan^2(\pi b/\lambda_0}\right] \qquad [28]$$

In order that the above relation may be satisfied

$$\tan^2(\pi nb/\lambda_0) < \tan^2(\pi b/\lambda_0) \qquad [29]$$

Or in other words, in order that the wire grid structure may simulate a plasma of electron density N, the dimensions a, b and d of the structure should be such that n remains less than unity for all angles of incidence θ. That is equation [29] and hence equation [28] sets the limit of a, b and d for which the simulation of plasma by artificial dielectrics can be achieved Similarly, in the case of a lossy plasma, the equivalent plasma density in terms of the structure parameters is obtained from equations [26] and [27] and $\omega_p^2=Ne^2/m$ and is given by the relation

$$N=\frac{m(\omega^2+\nu^2)}{e^2}\left[1-\frac{\tan^2(\pi nb/\lambda_0)}{\tan^2(\pi b/\lambda_0)}\right] \qquad [30]$$

In order that N may remain positive, the structure dimensions should be such that a remains less than unity.

7. EFFECT OF PLASMA ON RADIATION

The effects of interaction of plasma on microwave radiation are to shift the position of major lobe and also modify the shape of radiation patterns. The radiation patterns of a microvawe horn in free space and terminated in a ground plane are given by

$$E_\theta \propto \frac{\sin(\pi b/\lambda_0 \sin\theta)}{(\pi b/\lambda_0)\sin\theta} \qquad [31]$$

$$E_\phi \propto (\pi^2/4)\cos\theta\,\frac{\cos[(\pi a/\lambda_0)\sin\theta]}{[\pi a/\lambda_0)\sin\theta]^2-\pi^2/4} \qquad [32]$$

where, E_θ and E_ϕ refer to the patterns in the θ and ϕ planes respectively and θ and ϕ represent polar coordinates. The derivation of the above expressions for E_θ and E_ϕ assumes the existence of only the magnetic current sheet as the original electric current is cancelled by the electric current sheet in the image plane. In the presence of the plasma, however, the radiation from the horn induces surface currents in the plasma. If both the electric and magnetic current sheet distributions are taken into account, the radiation patterns of the horn with its ground plane embedded in plasma are given by the relations[16].

$$E_\theta \propto \left\{\frac{\sin(\gamma_0 b/2)\sin\theta}{(\gamma_0 b/2)\sin\theta}\right\}^2 \times \frac{1}{\cos^2(\gamma_p l) + (1/n^2)\left[(n^2-\sin^2\theta)/\cos^2\theta\right]\sin^2\gamma_p l} \quad [33]$$

$$E_\phi \propto \left\{(\pi^2/4)\cos\theta\frac{\cos\left[(\gamma_0 a/2)\right]\sin\theta}{(\pi^2/4)-\left[(\gamma_0 a/2)\right]\sin^2\theta}\right\}^2 \frac{1}{\cos^2(\gamma_p l)+\left[\cos^2\theta/(n^2-\sin^2\theta)\right]\sin^2\gamma_p l} \quad [34]$$

where, l represents the thickness of the plasma in the direction of propagation.

8. Experimental Radiation Patterns

The radiation patterns of pyramidal horns at X and K bands with and without plasma were obtained experimentally for a large number of wire grid structures simulating lossless and lossy plasma. The patterns were analysed with regard to the shift of the major lobe and distortion of the radiation patterns.

9. Results and Discussion

Some typical H-plane radiation patterns of a pyramidal horn with plasma sheaths simulated by wire grids at K band are shown in Fig. 3. The results are summarised in tables I, II and III.

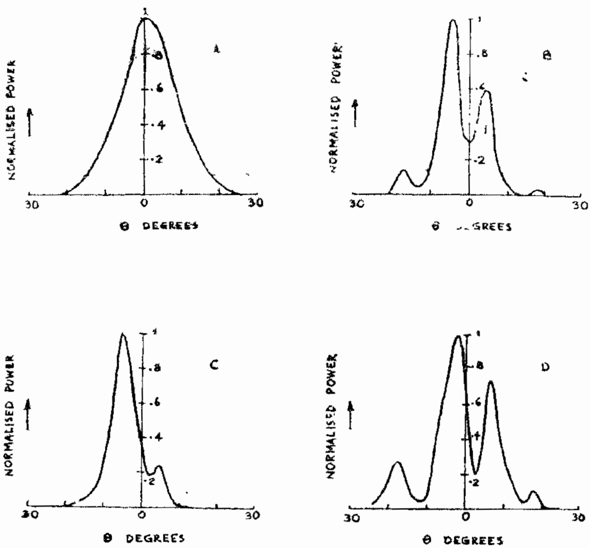

FIG. 3

H-Plane radiation pattern of pyramidal horn in the absence and presence of plasma at *K*-band.

A—Pyramidal horn

B—Horn with lossless *Y*—plasma ($b=6$ mm, $a=4$ mm)

C—Horn with lossless *XY* plasma ($b=5$ mm, $a=4$ mm)

D—Horn with lossy *Y* plasma ($b=10$ mm, $a=4$ mm)

TABLE I

Splitting and shift of the main beam at K band for lossless Y-plasma, $a=4$ mm.

b mm	No. of lobes	Magnitude of each lobe (normalised)	Position of each lobe with repect to the axis degrees	Direction of shift
3	Two	1.00	6	Anticlockwise
		0.6	5	Clockwise
4	Two	1.00	2	Anticlockwise
		0.78	8	Clockwise
5	Two	1.00	5	Anticlockwise
		0.60	6	Clockwise
6	Two	1.00	4	Anticlockwise
		0.60	4	Clockwise
9	Two	1.00	4	Anticlockwise
		1.00	5	Clockwise
10	One	1.00	4	Anticlockwise
11	Two	1.00	7	Anticlockwise
		0.90	2	Clockwise
12	Two	1.00	6	Anticlockwise
		0.80	3	Clockwise

TABLE 2

Splitting and shift of the beam at K band for lossless XY Plasma, $a=4$ mm

b mm	No. of Lobes	Magnitude of each lobe (normalised)	Position of each lobe with respect to the axis (degrees)	Direction of shift
2	One	1.00	6	Anticlockwise
3	One	1.00	4	Anticlockwise
4	One	1.00	4	Anticlockwise
5	One	1.00	6	Anticlockwise
6	Two	1.00	3	Anticlockwise
		0.88	3	Clockwise
7	Two	1.00	4	Anticlockwise
		0.66	5	Clockwise
8	Three	1.00	5	Anticlockwise
		0.84	1	Anticlockwise
		0.80	4	Clockwise
9	Two	1.00	6	Anticlockwise
		0.84	4	Clockwise
10	Two	1.00	6	Anticlockwise
		0.80	3	Clockwise
11	Two	1.00	5	Anticlockwise
		0.58	4	Clockwise
12	One	1.00	5	Clockwise
13	One	1.00	6	Clockwise

TABLE 3

Splitting and shift of beam at K band for Lossy Y plasma, $a = 4$ mm

b mm	No. of lobes	Magnitude of each lobe (normalised)	Position of each lobe with respect to axis (degrees)	Direction of shift
2	One	1.0	2	Anticlockwise
3	One	1.0	2	Anticlockwise
4	One	1.0	2	Anticlockwise
5	One	1.0	0	No shift
6	One	1.0	2	Clockwise
7	Two	1.0	3	Anticlockwise
		0.58	8	Clockwise
8	Two	1.00	3	Anticlockwise
		0.68	8	Ciockwise
9	Two	1.00	3	Anticlockwise
		0.92	6	Clockwise
10	Two	1.00	3	Anticlockwise
		0.78	6	Clockwise
11	One	1.00	2	Anticlockwise
12	One	1.00	1	Clockwise
13	One	1.00	0	No shift

The following observations may be made on the basis of the experimental sults on radiation patterns of a pyramidal horn in the presence of simulated asma at K band :

(i) The main beam is split into two components, the magnitude and shift of which are different in most cases.

(ii) For some values of b, the beam is not split but is shifted in the anticlockwise direction.

(iii) In the case of a lossy Y plasma there is no shift when $b = 5$ mm and $b = 13$ mm.

(iv) In the case of X band, the major lobe is shifted in the presence of both Y and XY plasma but no significant splitting of the beam was observed. Some typical experimental values of shift due to plasma at X band are given in Table 4.

TABLE 4

Shift of the major lobe at X band

b (cm)	Angle of shift in degrees for loseless Y plasma	b (cm)	Angle of shift in degrees for losseless XY plasma
Single sheath	2.5	Single sheath	0.5
0.9	2.0	0.9	1.0
2.7	1.5	1.8	4.0

The variation of shift (δ) with respect to normalised spacing b/λ_0 at $\lambda_0 = 1.25$ cm for lossless Y, XY and lossy plasma Y is shown in Fig. 4. The variation of equivalent plasma density with respect to b/λ_0 has been calculated from the observed angle of shift with the aid of the following relation

$$N = 1.242 \times 10^{-2} f_p^2 \, m^{-3} \qquad [35]$$

where the equivalent plasma frequency f_p is related to the refractive index n by the following relation

$$f_p^2 = f^2 (1 - n^2) \qquad [36]$$

and

$$n = \cos \delta \qquad [37]$$

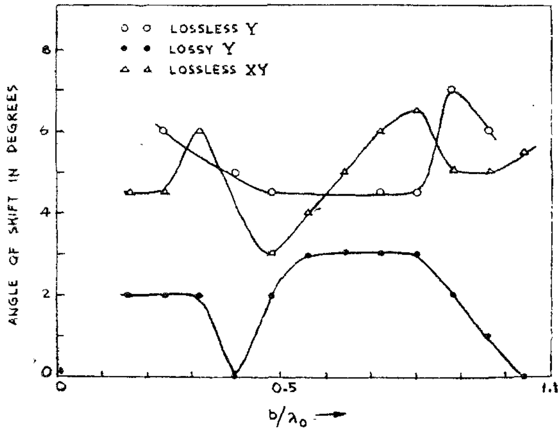

FIG. 4

Angle of shift δ vs b/λ_0, $a = 4$ mm at K band $\lambda_0 = 1\ 25$ cm.

The variation of equivalent plasma density with respect to the normalised spacing between two plasma sheaths for all the three types of plasma at K band is shown in Fig. 5.

The equivalent plasma density, refractive index as function of normalised spacing a/λ_0 between grid wire and corresponding angular plasma frequency ω_p and effective dielectric constant ϵ as function of a/λ_0 for various values of b/λ_0 for Y plasma calculated from the observed shift of the major lobe at X band are shown in Figures 6 and 7 respectively.

The equivalent lumped constants such as reactance X_g, shunt inductance L_p and impedance Z_s obtained from transmission line analogy have also been calculated as function of a/λ_0 for various values of b/λ_0 for losseless Y plasma at X band and the results are presented in Fig. 8. It is noticed that L_p increases but N decreases with increasing a/λ_0. This is probably due to the fact that as L_p increases, convection current decreases, consequently the equivalent plasma density decreases.

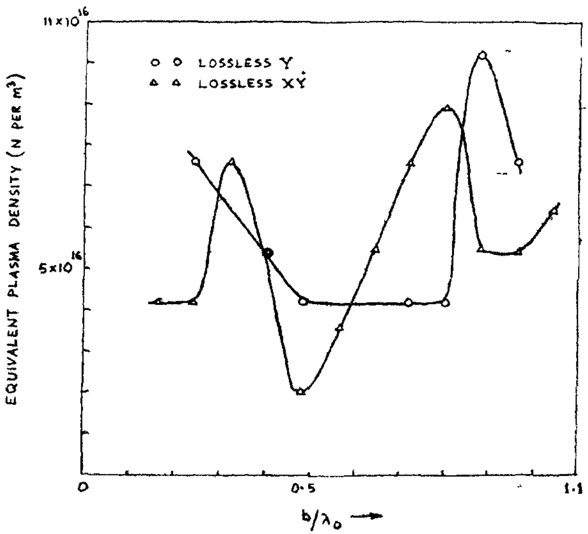

FIG. 5

Equivalent plasma Density vs b/λ_0 at K baud λ_0=1 25 cm a=4 mm

The half power beam widths of significant lobes vary with the normalised spacing b/λ_0. These variations at K band for all the three types of plasma shown in Figures 9 and 10 indicate that the variation is oscillatory in the case of beams which are shifted in the anticlockwise direction (Fig. 9) in cont·ast with the case of beams shifted in the clockwise direction (Fig. 10).

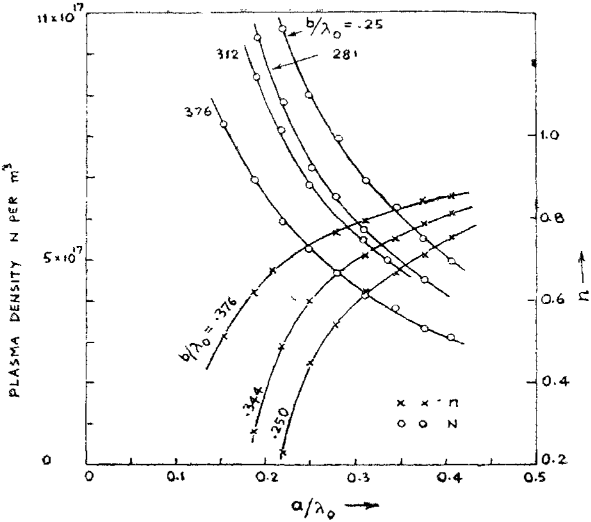

FIG. 6

Equivalent plasma Density and Refractive Index vs a/λ_0 at X band $\lambda_0=3.14$ cm.

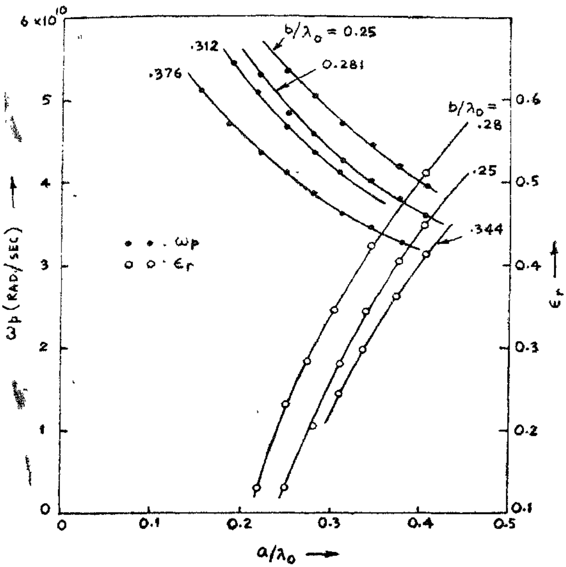

FIG. 7

ω_p and ϵ vs a/λ_0 at X band ; λ_0=3.14 cm.

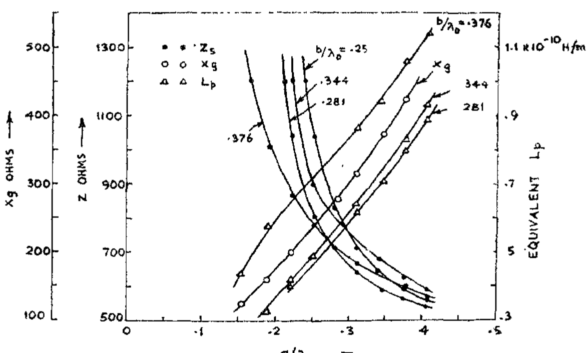

FIG. 8

Z_s, X_g, L_p vs a/λ_0 at Z band λ_0=3.14 cm.

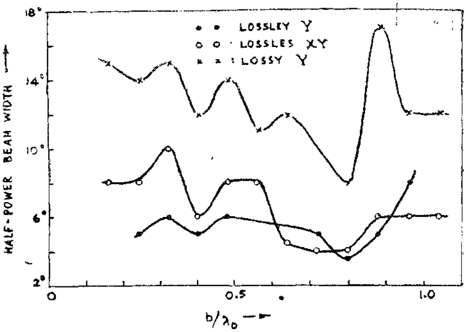

FIG. 9

Half-power beam width vs b/λ_0 for beams shifted anticlockwise at K band; $\lambda_0=125$ em, $a=4$ mm.

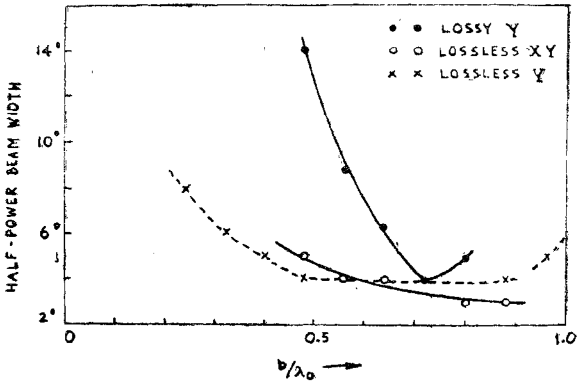

FIG. 10

Half power beam width vs b/λ_0 for beam shifted clockwise at K band. $\lambda_0=1.25$ cm, $a=4$ mm.

10. Reflection and Transmission Coefficients

The reflection ρ_w and transmission t_w coefficients in terms of b/λ_0 and a/λ_0 have been calculated by using equations [18] and [19] respectively where n is determined from the relation [12]. The variation of ρ_w and t_w with respect to b/λ_0 for a/λ_0 for lossless Y plasma at X band are shown in Fig. 11. The reflection (ρ_p) and transmission (t_p) coefficients have been calculated by using equations [20] and [21] respectively. The variations of ρ_p and t_p with respect to b/λ_0 for lossless Y and XY plasma at K band are shown in Figures (12) and (13) respectively. The variation of t_p and ρ_p with respect to a/λ_0 for different values of b/λ_0 at X band for lossless Y plasma are shown in Figures 14 and 15 respectively. Table 5 shows the difference between t_p and t_w at X band as function of b/λ_0 for $a/\lambda_0 = 0.376$.

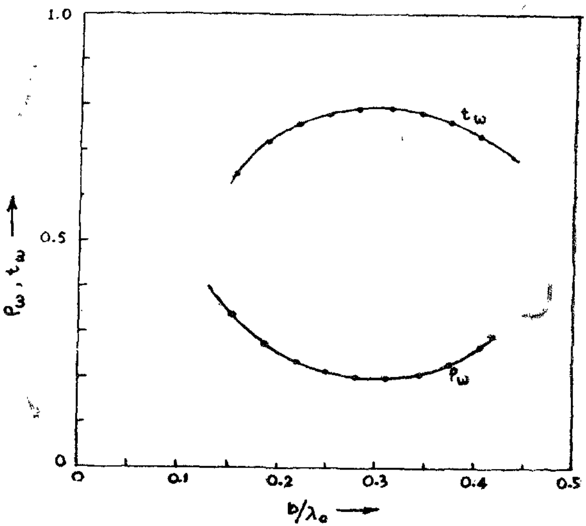

Fig. 11

Transmission (t_w) and reflection (ρ_w) coefficients vs b/λ_0 at X band, $a = 1.2$ cm. Lossless Y plasma

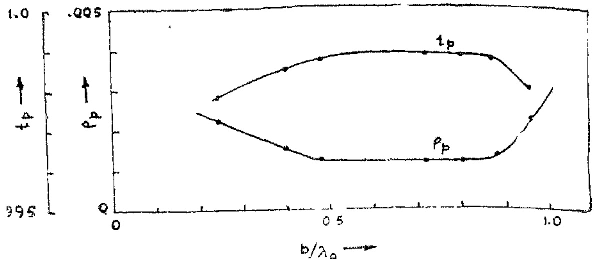

FIG. 12

Transmission (t_p) and reflection (ρ_p) coefficients as function of b/λ_0 at K band for Lossless Y plasma, a=4 mm.

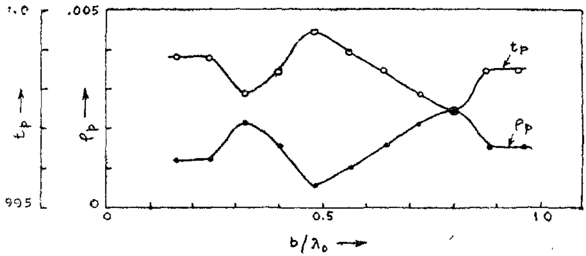

FIG. 13

Transmission (t_p) and reflection (ρ_p) coefficients as function of b/λ_0 for Losseless X-Y plasma K band.

TABLE 5

Difference in t_p and t_w at X band. a/λ_0=0.376

b/λ_0	$t_p - t_w$
0.250	0.047
0.281	0.068
0.312	0.08
0.376	0.14

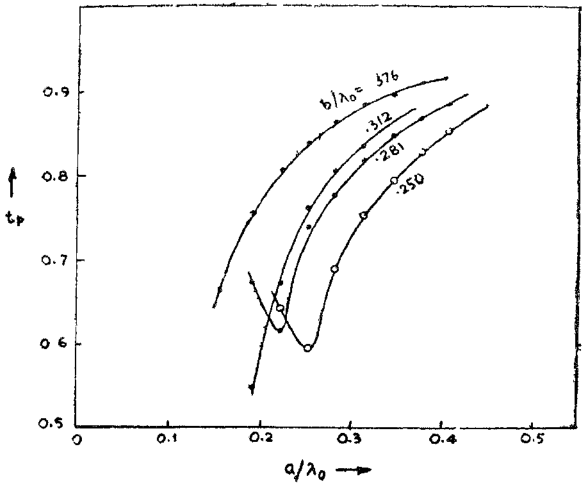

FIG. 14

Transmission (t_p) coefficient vs a/λ_0 for Losseless Y plasma at K band
(a) b/λ_0=0.250, (b) b/λ_0=0.281, (c) b/λ_0=0.312, (d) b/λ_0=0.376.

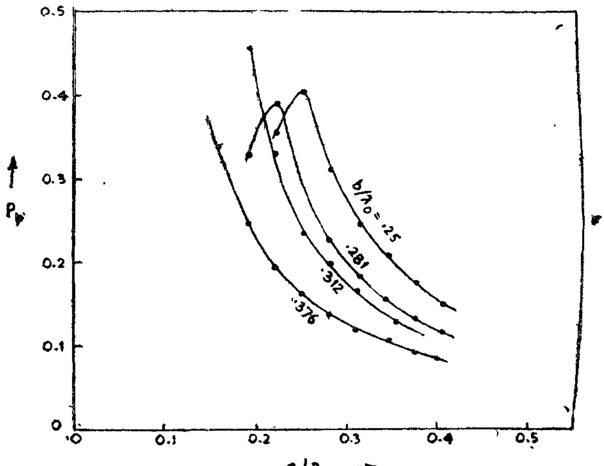

FIG. 15

Reflection (ρ_p) coefficient vs a/λ_0 for Lossless Y plasma
(a) b/λ_0=0.250. (b) b/λ_0=0.281. (c) b/λ_0 =0.312. (d) b/λ_0=0.376.

The difference $t_h - t_w$ is probably due to the diffraction effects which have not been taken into account in deriving the relation for n which is used in calculating the values of t_{th}.

11. ACKNOWLEDGEMENT

The authors express their thanks to the Professor-in-charge for the facilities provided during the course of the investigations.

REFERENCES

1. Carlson, J. F. and Heins, A. E. .. *Q. Appl. Math.* 1947, **4**, 313.
2. Chatterjee, S. K and Vasudeva Rao, B. *J. Indian Inst. Sci* , 1955, **37**, 304.
3. Charterjee, S. K., (Mrs.) Chatterjee, R. and Sunderrajan, D. *J. Instn. Engrs. India*, 49, ET-1, 9, 196.
4. Wait, J. R. .. .. *Appi. scient. Res.* 1954, **B4**, 393.
5. Brown, J. .. .. *Proc. Instn. elect. Engrs.*, 1953, **100**, 51.
6. Macfarlane. G. G. .. .. *Ibid*, 1946, **3A**, 93, 1523.
7. Ignatousky, W. .. .. *Annln. Phys.*, 1914, **44**, 369.
8. ——— .. .. *HochfreqTech Electroakust*, 1939, **54**, 62.
9. Skwirzyriski, J. K., Thackray, J. C. .. *Marconi Rev.*, 1959, **22**, 77.
10. Chatterjee, S. K. and (Miss) Dhanalakshmi, C. .. .. *Z. Phys.*, 1960, **158**, 196.
11. ——— .. .. *J. Instn. Telecommun. Engrs.*, 1960, **6**. 149.
12. ——— .. .. *Ibid*, 1960, **6**, 83.
13. Bracewell, R. N. .. .. *Wireless, Engr.*, 1954, **31**, 320.
14. Baker, W. G. and Ria, C. W. .. *Trans. Am. Inst. elect. Engrs.*, 1926. **45**, 302.
15. Rotman, W. .. .. *I.R.E. Trans. Antennas Propag.*, 1962, **AP-10**, 82.
16. Elliot, R. S. and Flock, W. L. .. *Ibid*, 1962, **AP-10**, 65.